CONSTRUCTAL DESIGN OF MOLTEN SALT FLOW AND HEAT TRANSFER IN HORIZONTAL HOLLOW DISC-SHAPED HEATERS

Wei FU [*], Hua LIN[**], Xinzhi LIU[*], Houlei ZHANG[*]

[*] Nanjing University of Science and Technology, Xiaolingwei 200, Nanjing 210094, China
[**] Xishuangbanna Tropical Botanical Garden, Chinese Academy of Sciences, Mengla 666303, China
Corresponding author: Houlei ZHANG, E-mail: `houlei_zhang@aliyun.com`

Abstract. Molten salt-based horizontal hollow disc-shaped heaters important in material heating fields were studied. By invoking constructal design method, we investigated the effects of inlet/outlet structures, internal circumferential fins and guiding plates on molten salt flow and heat transfer. The hot air pre-heating time in cold-start process was also documented. The results show that bottom surface-positioned inlet/outlet structures provide better heat transfer performance and less entropy generation rate than side surface-positioned designs. Inlet/outlet structures with larger volumes generate smaller pressure drop. Increasing fin number can improve flow and heat transfer performance simultaneously for specified cases. Guiding plates increase both the heat transfer coefficient and the pressure drop. Better heat transfer design also shortens the pre-heating time that is good for dynamic process control.

Key words: Molten salt, disc-shaped heater, constructal design, heat transfer, entropy generation.

1. INTRODUCTION

Disc-shaped heater (Fig. 1) is a kind of indirect heating equipment that is widely used in material drying [1]. It is composed of some static hollow discs with central holes. In the hollow discs, the hot working fluid (heat transfer oil or steam) flows from inlet to outlet and transfers heat to the outside material via the top surfaces of the discs. In many material thermal processing applications (e.g., biomass pyrolysis), where the temperature is in the range 300℃–600℃, molten salt becomes favourable. Recently, Vignarooban et al. [2] reviewed heat transfer fluids (including molten salts) thoroughly for concentrating solar power systems and Du *et al*. [3] reviewed high temperature molten salt heat exchangers and their applications in both conventional industrial heating and renewable energy fields. When the material-side convective heat transfer coefficient is in the same scale as that of the working fluid-side, it is important to enhance the heat transfer of both sides. For disc-shaped dryers with radial fin design, Zhang *et al*. [4] presented numerical and experimental results using hot water as the working fluid. Pin fins were also developed to enhance heat transfer in hollow discs [1]. Since the Constructal Law was proposed by Bejan [5], constructal design method (CDM) has been extensively utilized in flow and heat transfer design and optimization [6–7]. Recently, Zhang [8] investigated the molten salt flow and heat transfer characteristics in hollow paddle-shaft structures based on CDM. They revealed the design evolving direction of the paddles and heat transfer effect of internal guiding plates.

According to the Constructal Law, with specified material-side constraints, one way to enhance the molten salt-side heat transfer is to distribute the fluid and bathe the internal space of the hollow discs as uniformly as possible. Along this way, in this paper, we will study the steady and dynamic heat transfer processes of molten salt in hollow disc-shaped heaters and search better designs for potential applications.

2. NUMERICAL MODEL

Consider one hollow disc with Hitec salt (53% KNO_3 – 40% $NaNO_2$ – 7% $NaNO_3$ based on mass fraction) as the working fluid, shown in Fig. 2. There are two common types of inlet/outlet structures to be

selected. One is side surface-positioned (Fig. 2 right half) and another is bottom surface-positioned (Fig. 2 left half). The effects of guiding plates and circumferential fins in the hollow disc are to be further discussed. As molten salt will solidify when its temperature is lower than its melting temperature, the dynamic behaviour (e.g., cold-start process) will be investigated. We will simulate the molten salt flow and heat transfer processes by using CFD model for three-dimensional conjugated heat transfer. Assume that the molten salt flow is incompressible and turbulent, the properties of fluids and stainless steel are constant except the air density in natural convection in dynamic simulations, and the influence of gravity is negligible.
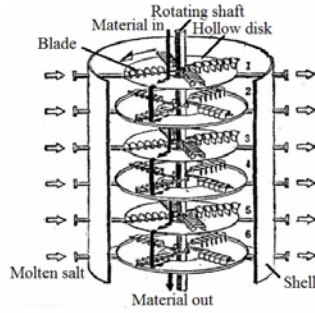

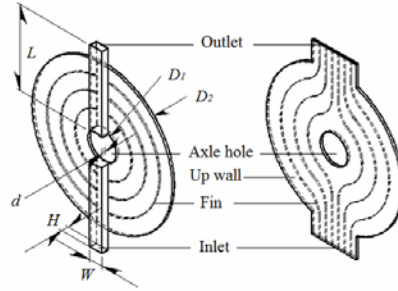Fig. 1 – Configuration of disc-shaped heater [1].

Fig. 2 – Computational domain of hollow disc-shaped heater: D_1 = 500 mm, D_2 = 2500 mm, L = 1300 mm, d = 41 mm, H – variable, W - variable, thickness of walls and fins = 8mm.

For steady analysis, standard k-ε turbulence model is used to simulate molten salt flow and heat transfer and transient heat conduction equation without heat generation is used to calculate the heat transfer in solid. All equations can be easily found from standard textbooks, e.g., [9]. Effective convective heat transfer coefficient h_{eff} is defined as $h_{eff} = QA\Delta T_{ave}$, where Q is heat transfer rate, A is the top surface area of the hollow disc and ΔT_{ave} is average temperature difference. In the dynamic simulations, we only consider the cold-start process in which hot air on the outside of the disc is used to heat the device with trapped air in the hollow disc. The objective is to determine the pre-heating time that prevents liquid salt solidification. The trapped air is simulated with standard natural convection k-ε turbulence model [9]. The radiation between solid surfaces is included in the model. Based on simulation results, the entropy generation rate S_g is given as follows [10]

$$S_g = \dot{m}\left(s_{out} - s_{in}\right) + \dot{Q}/T_0 = \dot{m}c_p \ln T_{out}/T_{in} + \alpha V \Delta P \rho + \dot{Q}/T_0 \ . \tag{1}$$

In Eq. (1), m is mass flow rate, s_{in} and s_{out} are inlet entropy and outlet entropy respectively, T_o is material temperature, c_p is specific heat, T_{in} and T_{out} are inlet temperature and outlet temperature respectively, α_V is thermal expansion coefficient, ΔP is pressure drop and ρ is density. The boundary conditions for steady simulations are given as follows: T_{in} = 550°C, specified pressure at molten salt outlet, T_o = 400°C and material-side convective heat transfer coefficient h_o = 200 W/(m²·K). The boundary conditions and initial conditions for dynamic simulations are given as follows: adiabatic wall at inlet and outlet, radiation heat transfer coupled internal walls with emissivity 0.8, air temperature 400°C, external air convective heat transfer coefficient 50 W/(m²·K) and external solid surface emissivity 0.8. The properties of Hitec salt are obtained based on [11]. The density, specific heat and thermal conductivity of stainless steel are 7 980 kg/m³, 485 J/(kg·K) and 21 W/(m·K) respectively. The inlet and outlet arrangements are symmetrical and listed in Table 1.

To solve the flow and temperature fields a finite-volume computational package ANSYS Fluent with pressure-based solver SIMPLE algorithm was used [12]. Second-order upwind scheme was used for convection terms in spatial discretization. The residuals for continuity, momentum are 10^{-3} and the residual for energy is 10^{-6}. The space and time mesh independence was checked before each simulation was performed. Less than 1% changes in pressure drop, heat transfer rate and pre-heating time between successive meshes are considered acceptable results. The number of space grids used in the simulations varies from case to case, from a few million to more than twenty million. Dimensionless mass flow rate M, pressure drop Be, effective heat transfer coefficient h_{eff} and entropy generation rate S_g are used to summarize the simulating results: $M = mh_0 A/c_p$, $\mathrm{Be} = \Delta P D^2/\mu\alpha$, $\tilde{h}_{eff} = h_{eff}/D_2\lambda$, $\tilde{S}_g = \dot{S}_g/\left(h_0 A\left(T_{in} - T_0\right)/T_0\right)$, where μ is dynamic viscosity and a is thermal diffusivity [11].

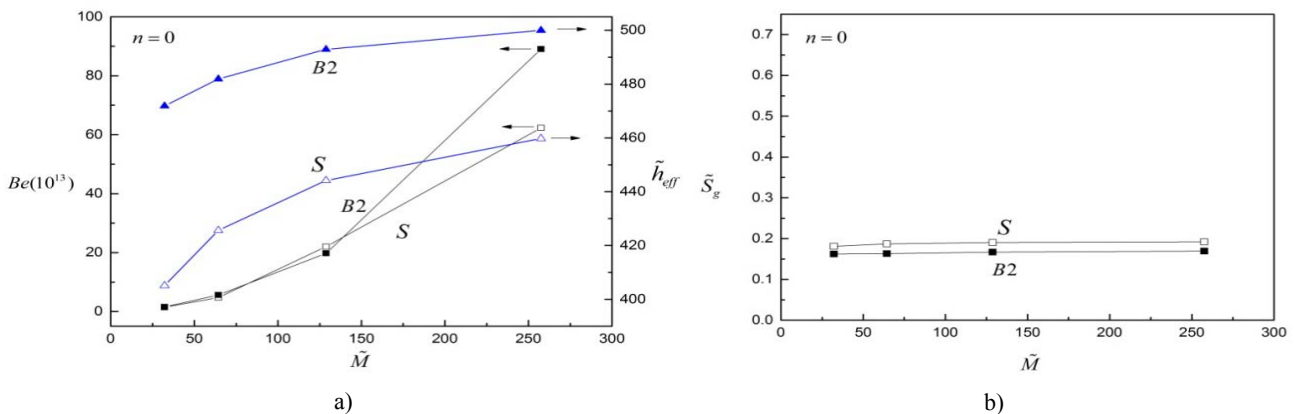*Table 1*

The inlet and outlet structures

Position	Inlet/outlet cross sectional area [H×W]	Guiding plate	Design symbol
Bottom surface-positioned	100 mm × 100 mm	No	*B1*
	100 mm × 200 mm	No	*B2*
	150 mm × 200 mm	No	*B3*
	200 mm × 200 mm	No	*B4*
	100 mm × 200mm	Yes	*B2G*
Side surface-positioned	25 mm × 800 mm	No	*S*
	25 mm × 800 mm	Yes	*SG*

3. RESULTS AND DISCUSSION

For flat hollow disc heaters, both side surface-positioned and bottom surface-positioned inlet/outlet structures are possible. The former structure is usually constrained by the height of the hollow disc and the latter structure can distribute the inlet flow uniformly. Figure 3 shows a comparison example of these two structures with specified inlet cross sectional area. The heat transfer coefficient of *B2* is obviously greater than that of *S*. When the mass flow rate is low, the pressure drop gap between *B2* and *S* is tiny. When the mass flow rate is large ($M > 150$), the pressure drop of *B2* is larger than that of *S*. Figure 4 gives the velocity and temperature fields. It can be seen that more space is bathed by the molten salt in *B2* than in *S*. From Fig. 3b, the entropy generation rate of *B2* is less than that of *S* in the specified mass flow rate range which indicates *B2* is better than *S* from the view of irreversibility minimization.

a)   b)

Fig. 3 – A comparison example of *B2* and *S* inlet/outlet geometry.

In many cases of constructal designs, the fluid volume was fixed. In real designs, if the volume price is cheap or acceptable, we can relax this volume constraint to search better performance. In Fig. 5, the performance of four bottom surface-positioned inlet/outlet structures with different inlet/outlet volumes is presented. When the inlet/outlet volume increases, the pressure drop decreases significantly (Fig. 5a). This pressure drop decrease also brings about the decrease of the entropy generation rate (Fig. 5b). In practical design, if space is permitted, larger inlet/outlet volume is recommended. The corresponding manufacture cost increase is in fact negligible.

Besides choosing proper inlet/outlet structures, we introduced internal circumferential fins to enhance the molten salt heat transfer. Assume the fins are equidistant. Figure 6 shows the effects of fin number (*n*). With the increasing in *n*, the heat transfer coefficient increases and the pressure drop decreases. Commonly, more fins mean more friction, so the present positive observation indicates that the flow field with more fins is better than that with less fins. The fins guide the fluid toward easier flow access. In the present example in Fig. 6, the entropy generation rate change is quite limited.
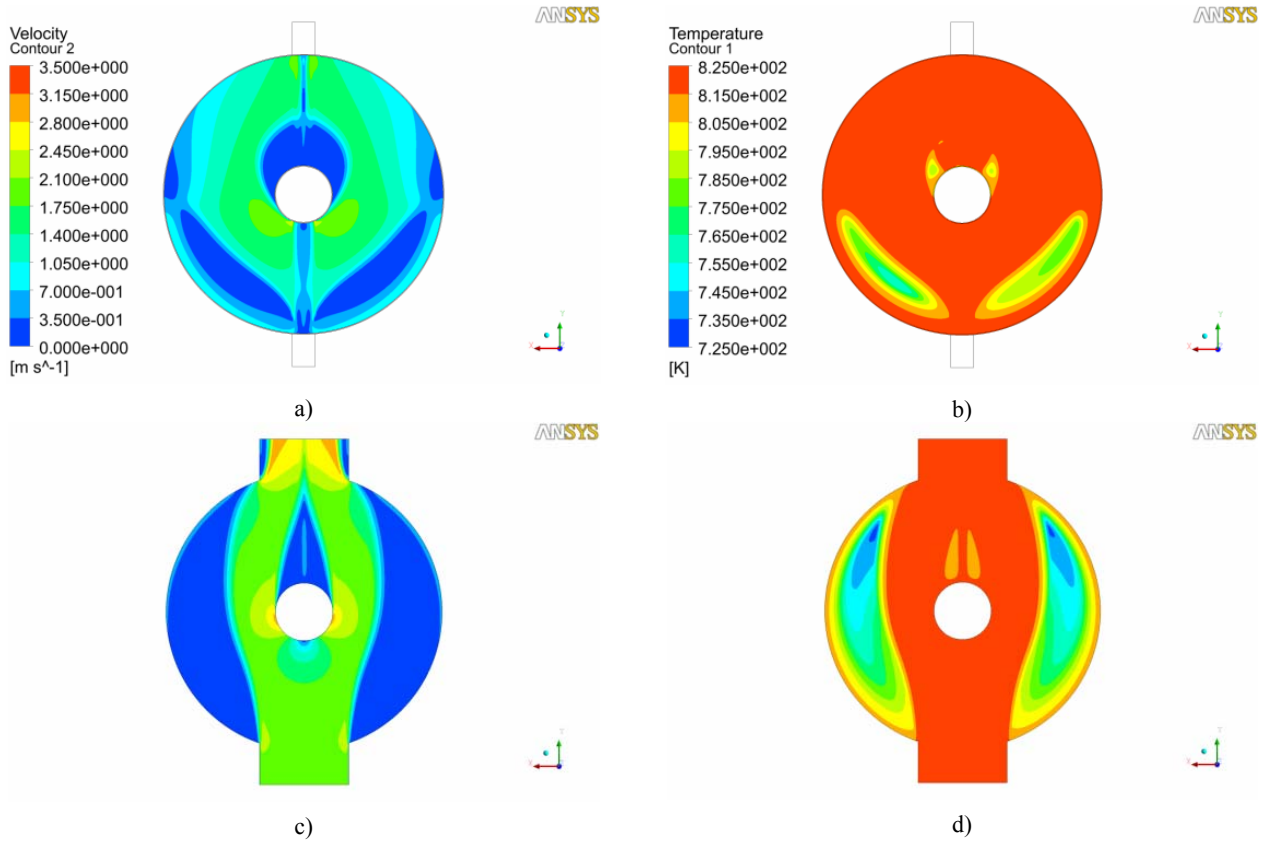
Fig. 4 – The velocity field (the central cross section in the thickness direction) and the temperature field (top surface) of *B2* and *S* with *n* = 0 (*M* = 128.77): a) *B2*, velocity field; b) *B2*, temperature field; c) *S*, velocity field; d) *S*, temperature field.
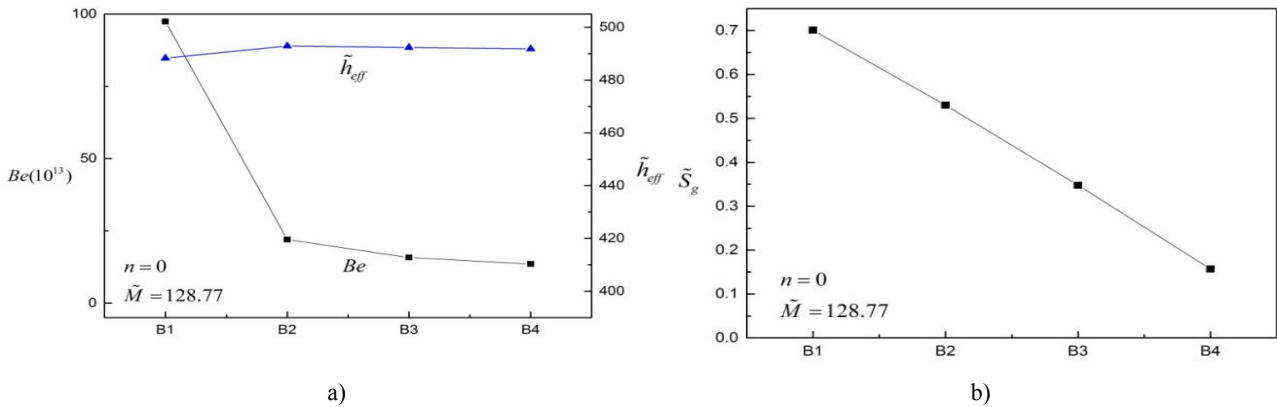

Fig. 5 – The effects of inlet/outlet volume.

Figure 7 presents the effects of fin pitch (represented by diameter *D*) for *B2* with *n* = 1, where $r = (D–D_1)/(D_2–D_1)$. The effects of *r* on both flow and heat transfer are not obvious for the specified mass flow rate. When *r* = 0.125, the heat transfer coefficient and the entropy generation rate are a little bit higher. The effects of more fins with other flow rates can be analyzed similarly.

For both side surface-positioned and bottom surface-positioned inlet/outlet designs, the flow and heat transfer in the hollow disc can be further modified by introducing guiding plates. Figure 8 illustrates the effects of guiding plates. Both the heat transfer coefficient and pressure drop of *B2G* with guiding plates are greater than that of *B2*. This indicates that better heat transfer in the hollow disc is accompanied by the significantly enlarged inlet/outlet pressure drop due to smaller cross sectional area of the inlet/outlet structures induced by guiding plates. The performance of *SG* is also presented in Fig. 8. Seen in Fig. 8b, the entropy generation rates of *B2G* and *B2* are nearly the same but larger than that of *SG*.
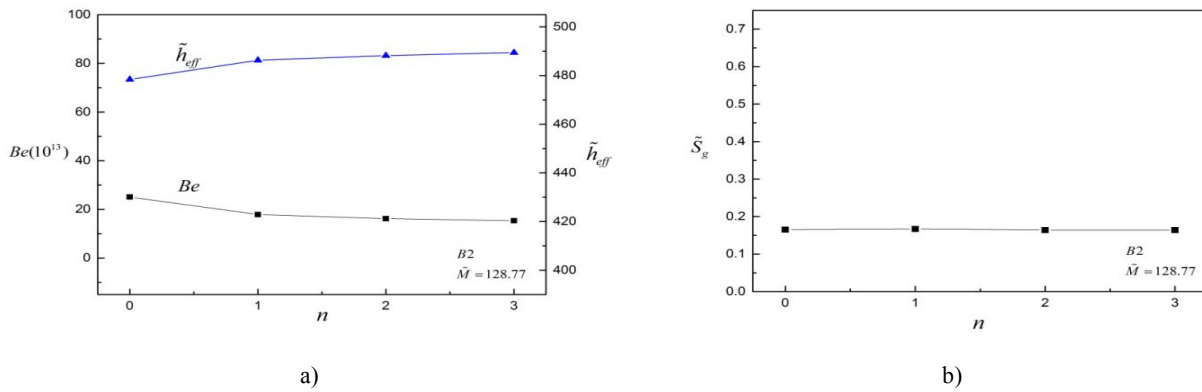
a)

b)

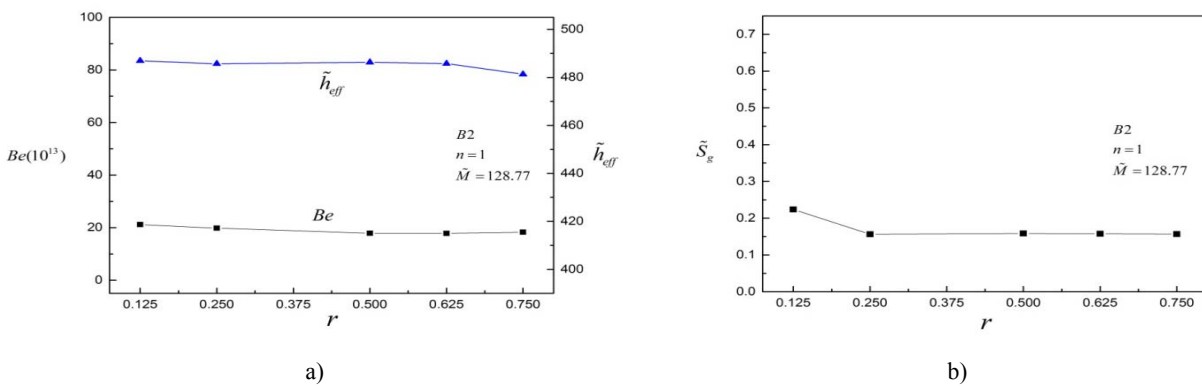Fig. 6 – The effects of fin number.

a)

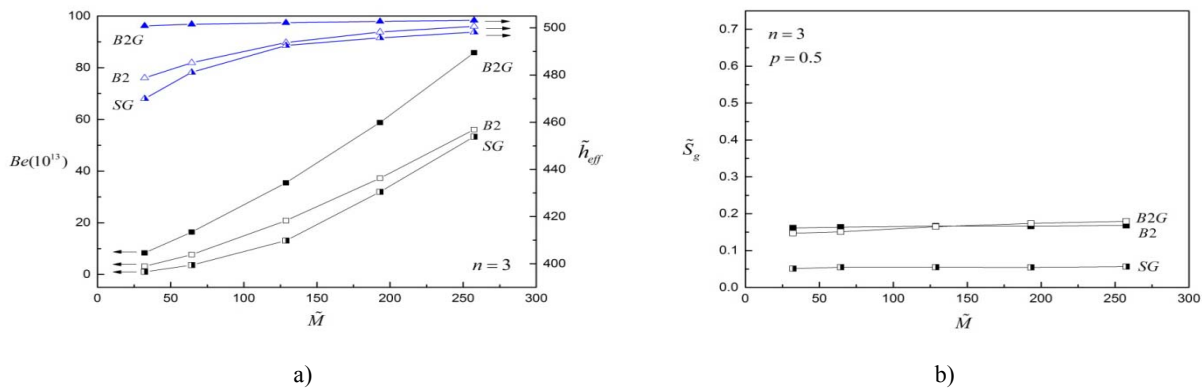b)

Fig. 7 – The effects of fin pitch.

a)

b)

Fig. 8 – The effects of guiding plates.

In order to prevent salt solidification in the cold-start process, the pre-heating process with hot air as the pre-heating medium should sustain until the minimum solid temperature T_{min} is higher than the melting temperature (142°C or 415K for Hitec salt). After that, molten salt is pumped into the hollow discs of the heater. Figure 9 documents temperature rising curves of two designs in the cold-start process. The pre-heating time is about 390s for the design $B2G$ with $n = 3$ and 720s for the design $B2$ with $n = 0$ respectively. The result shows that the enhanced heat transfer design also shortens the cold-start time efficiently. Based on the relationship between the air temperature T_{air} and the minimum solid temperature T_{min}, the air temperature can be monitored for cold-start process control which is more convenient.
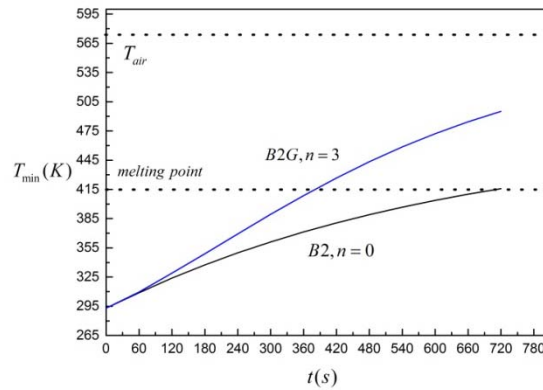
Fig. 9 – Temperature rising curves in cold-start pre-heating process.

4. CONCLUSIONS

We investigated the flow and heat transfer performance in the hollow disc-shaped heaters. By invoking constructal law, we analyzed the performance influencing factors such as inlet/outlet structures, circumferential fins and guiding plates. The bottom surface-positioned inlet/outlet structure is better than side surface-positioned structure from the heat transfer view and the entropy generation rate view. Larger inlet/outlet volume helps to decrease pressure drop. Case study shows that increasing fin number can improve flow and heat transfer performance simultaneously. The inlet/outlet guiding plates increase the heat transfer coefficient and the pressure drop at the same time. The present study demonstrates a constructal design example that by evolving the internal geometry of horizontal hollow discs the performance can be improved. More optimization space still exists.

REFERENCES

1. Y. PAN, X. WANG, X. LIU, *Modern Drying Technology* (in Chinese), Chemical Industry Press, 2006.
2. K. VIGNAROOBAN, X. XU, A. ARVAY, K. HSU, A.M. KANNAN, *Heat transfer fluids for concentrating solar power systems – A review*, Applied Energy, **146**, pp. 383–396, 2015.
3. J. DU, F. SHAO, W. DU, H. ZHANG, X. LIU, *Review on high temperature molten salt heat exchangers and applications* (in Chinese), Solar Energy, **8**, pp. 35–40 and 55, 2015.
4. L. ZHANG, N. MA, J. LIU, Z. ZHANG, X. SUN, *Simulation and experiment on temperature field of dial dryer with radicalized internal flow passages* (in Chinese), Chemical Engineering, **43**, *12*, pp. 16–20, 2015.
5. A. BEJAN, *Constructal-theory network of conducting paths for cooling a heat generating volume*, Internal Journal of Heat and Mass Transfer, **40**, *4*, pp. 799–816, 1997.
6. A. BEJAN, S. LORENTE, *Design with Constructal Theory*, John Wiley & Sons, 2008.
7. A. BEJAN, *Evolution in thermodynamics*, Applied Physics Reviews, **4**, *1*, 011305, 2017.
8. K. ZHANG, J. DU, X. LIU, H. ZHANG, *Molten salt flow and heat transfer in paddle heat exchangers*, International Journal of Heat and Technology, **34**, S1, pp. S43–S50, 2016.
9. W. TAO, *Numerical Heat Transfer* (in Chinese), 2nd ed., Xi'an Jiaotong University Press, 2001.
10. W. SHEN, J. TONG, *Engineering Thermodynamics* (in Chinese), 4th ed., Higher Education Press, 2007.
11. COASTAL CHEMICAL Co., *HITEC® Heat Transfer Salt*, pp. 1–10.
12. FLUENT INC., *ANSYS Fluent, User's Manual* (version 14.0).